Science of the Total Environment 806 (2022) 151347

Contents lists available at ScienceDirect

Science of the Total Environment

journal homepage: www.elsevier.com/locate/scitotenv

Development of a cold-start emission model for diesel vehicles using an artificial neural network trained with real-world driving data

Jigu Seo [a], Boseop Yun [b], Juwon Kim [b], Myunghwan Shin [b], Sungwook Park [c,*]

[a] Graduate School of Hanyang University, 222 Wangwimni-ro, Seongdong-gu, Seoul 04763, Republic of Korea
[b] National Institute of Environmental Research, Hwangyong-ro 42, Seo-gu, Incheon 22689, Republic of Korea
[c] Department of Mechanical Engineering, Hanyang University, 222 Wangwimni-ro, Seongdong-gu, Seoul 04763, Republic of Korea

HIGHLIGHTS

- Artificial neural network-based cold start emission model was developed.
- Real-world driving data were used to train artificial neural network.
- Proposed model predicted a sharp increase in exhaust emissions after a cold start.
- Exhaust emissions according to engine temperature were visualized in emission map.

GRAPHICAL ABSTRACT

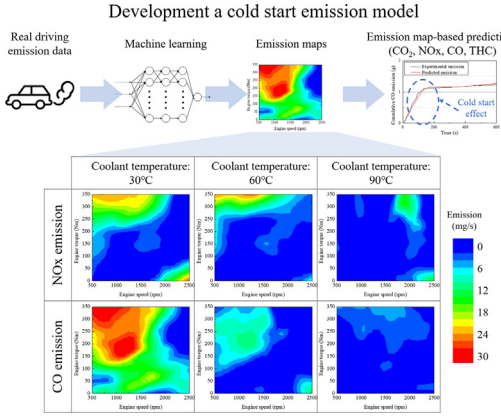

ARTICLE INFO

Article history:
Received 31 August 2021
Received in revised form 20 October 2021
Accepted 27 October 2021
Available online 30 October 2021

Editor: Pavlos Kassomenos

Keywords:
Vehicle emission model
Cold start emission
Artificial neural network
Real driving emission
Emission map

ABSTRACT

During the cold start and warm-up phase, modern vehicles emit considerable amounts of pollutants due to the incomplete combustion and deteriorated performance of aftertreatment devices. In terms of emission modeling, there have been many attempts to estimate cold start emission such as cold-hot conversion factor, regression model, and physis-based model. However, as the emission characteristic become complicated due to the adoption of aftertreatment devices and various emission control strategies for the strengthened emission regulations, the conventional cold start emission models do not always show satisfactory performances. In this study, artificial neural networks were used to predict the cold start emissions of carbon dioxide, nitrogen oxides, carbon monoxide, and total hydrocarbon of diesel passenger vehicles. We used real-world driving data to train neural networks as an emission prediction tool. Through machine leaning, numerous trainable variables of neural networks were properly adjusted to predict cold start emissions. For input variables of the ANN model, the velocity, vehicle specific power, engine speed, engine torque, and engine coolant temperature were used. The proposed ANN models accurately predicted sharp increases in carbon monoxide, hydrocarbon, and nitrogen oxides during the cold start phase. In addition to the quantitative estimations, the correlations between the operating variables and exhaust gas emissions were visually described in the form of emission maps. The emission map graphically showed the emission levels according to the vehicle and engine operating parameters.

Abbreviations: ANN, Artificial Neural Network; CO, Carbon Monoxide; CO_2, Carbon Dioxide; DOC, Diesel Oxidation Catalyst; DPF, Diesel Particulate Filter; LNT, Lean NOx Trap; NOx, Nitrogen Oxides; OBD, On-Board Diagnostics; PEMS, Portable Emission Measurement System; RDE, Real Driving Emission; SCR, Selective Catalytic Reduction; THC, Total Hydrocarbon; HC, Hydrocarbon; VSP, Vehicle Specific Power.

* Corresponding author at: Department of Mechanical Engineering, Hanyang University, 17 Haengdang-dong, Seongdong-gu, Seoul 133791, Republic of Korea.
E-mail address: parks@hanyang.ac.kr (S. Park).

https://doi.org/10.1016/j.scitotenv.2021.151347

1. Introduction

For modern vehicles, the additional exhaust emissions during the cold start phase have become a critical issue in transportation-related air pollution. In cold start conditions, vehicles emit significantly more pollutant than in hot driving conditions due to unfavorable thermal conditions for emission control. The thermal conditions of the engine and aftertreatment devices have a significant impact on exhaust emissions. During the cold start phase, the low temperature of the engine leads to several problems, such as imperfect fuel evaporation, an increased fuel film, and the need to consider fuel-enrichment strategies for proper drivability, resulting in low combustion efficiency and increased exhaust emissions (Bielaczyc and Merkisz, 1997; Roberts et al., 2014). In addition, the conversion efficiency of aftertreatment devices was deteriorated at low temperatures. Since most aftertreatment devices utilize catalytic reactions for pollutant reduction, their pollutant reduction performance is unsatisfactory under the light-off temperature (Gao et al., 2019; Bielaczyc et al., 2011).

In recent years, cold start emissions have accounted for a large portion of vehicle emissions. In contrary to hot running emissions, which have continuously decreased as a result of the tightened emission regulations and technology developments, cold start emissions have not effectively reduced over the last few decades. (Weilenmann et al., 2009; Favez et al., 2009). Although the cold start phase accounts for only 15% of the total driving time of the New European driving cycle (NEDC) test, carbon monoxide (CO) and hydrocarbon (HC) emissions in the cold start phase account for up to 80% of the total emissions (Robinson et al., 2013). In read-driving tests, most of the CO and HC emissions were emitted during the cold start phase when the engine was not fully warmed up (Du et al., 2020; Weilenmann et al., 2009). In addition to CO and HC, nitrogen oxide (NOx) emissions were also increased under the cold start condition due to the degraded performance of NOx aftertreatment devices at low temperatures (Dardiotis et al., 2013).

In terms of emission modeling, many attempts have been made to estimate cold start emissions. Conventional cold start emission models can be classified according to their modeling approaches. Applying cold start conversion factors to hot emissions is the simplest and widely used method for estimating cold start emissions (Gkatzoflias et al., 2007; Joumard et al., 2007). Conversion factors were often composed of empirical functions, which were obtained through statistical process comparing hot emissions and cold emissions based on a large amount of experiment data. In addition to simple conversion factors, detailed modeling approaches also have been used to predict cold start emissions. Giannelli et al. (2014) estimated cold start emissions using a semi-empirical method that operated as a function of the vehicle tractive power. This model considered the impacts of vehicle power and catalyst warm-up time on cold start emissions. Favez et al. (2009) investigated the relationship between the stop time and cold start emissions. They quantified the relative extra emissions according to a range of stop times (from 0 to 12 h). Sabatini et al. (2015) proposed a semi-empirical model to calculate the temperature of the catalytic converter. This model can predict the time it takes to reach the light-off temperature of the catalyst during the cold start. Weilenmann et al. (2013) developed a simplified physics-based model to predict cold start emissions. This model showed reliable prediction accuracy under various driving pattern, ambient temperature, and stop time conditions.

However, as vehicle technologies improve to meet strengthened emission standards such as real driving emission (RDE) regulations, emission characteristics under cold start conditions have become more complicated and diversified depending on the vehicle and emission types (Franco et al., 2013). The aftertreatment devices and various engine control strategies of modern vehicles made cold start emission characteristics further complicated (Neely et al., 2014; Neely et al., 2013).

As the emission characteristic become complicated, the conventional cold start emission models do not always show satisfactory performances. Both conventional empirical model and physics-based model have the limitations in estimating cold start emissions of various modern vehicles. Since empirical models are based on a relatively simple statistical process, the prediction accuracy for cold start emissions is not satisfactory. On the contrary, implementation of physics-based model required detailed information such as detailed specifications for engine and aftertreatment devices and their control algorithms, which may become an obstacle for model development.

Much research in recent years has focused on ANNs to model and predict exhaust emissions. Sharma et al. (2005) evaluated the performance of ANN-based vehicular emission models. The prediction accuracies of ANN-based emission models were satisfactory due to their ability to model nonlinear characteristics. Hashemi and Clark (2007) predicted carbon dioxide (CO_2), NOx, HC, and CO emissions of heavy-duty vehicles by using an ANN model as a predictive tool. Their proposed ANN model used the axle rotational speed and axle torque (and their derivatives) as model input variables to predict target emissions. Jaikumar et al. (2017) developed an ANN-based, real-time emission model for a passenger car. Through parametric study, they analyzed which variables were effective as ANN inputs for emission prediction. The proposed model used the vehicle speed, acceleration, engine speed, and vehicle specific power (VSP) as input variables. Inclusion of other parameters as ANN inputs, such as the oil temperature, engine load, intake air temperature, and throttle position, showed only a marginal improvement for emission predictions. Le Cornec et al. (2020) developed an instantaneous NOx prediction model based on an ANN trained with large amount of real-world driving data. The proposed model showed satisfactory NOx prediction accuracy with a relatively simple variables such as vehicle speed and acceleration. Wang et al. (2018) predicted the CO_2, CO, NOx, and HC emissions for different fuel types using vehicle specific power-based ANN model. The proposed ANN model showed better performance in emission predictions compared to regression model in all indicators such as mean absolute percentage error, root mean squared error, and mean absolute error.

In order to predict cold start emission with high performance, this paper presents a novel and reliable methodology to predict cold start emissions based on artificial neural networks (ANNs). Since ANNs consist of nonlinear functions and numerous trainable variables, which can be adjusted to predict the target value through machine learning, this methodology can effectively take into account the complex and nonlinear behavior contained in the training data. In addition, ANN-based models do not require high level of modeling techniques which was essential for conventional physics-based emission model. By properly designing ANN structure, ANNs can train the emission characteristics of the experiment data by themselves through machine learning. Currently, many real-world driving tests are being conducted around the world for regulatory purposes (Gao et al., 2021). Therefore, more experimental data will be available for development of ANN models.

In this study, we predicted cold start CO_2, NOx, CO, and total hydrocarbon (THC) emissions using ANNs, which were trained with real-world driving data. Four types of ANN models were developed for each exhaust species depending on the combination of input variables such as velocity, VSP, engine speed, engine torque, and engine coolant temperature. Through the machine learning, ANN model trained the correlation between the operating variables and exhaust emissions represented in experimental data. The emission prediction accuracies of developed ANN models were validated by comparing with experiment emissions. In addition, since the ANN model is a black box model, we introduced emission maps to describe the emission characteristics trained in these ANN models. We visualized cold start emissions according to the engine coolant temperature in the form of an emission map.

2. Methodology

2.1. Artificial neural network model

In order to achieve optimal performance of ANN models, multiple types of ANN models were developed, and their prediction accuracies were compared. We developed four types of 'multi-layer, feed-forward neural network' models, as shown in Fig. 1. A total of five operating variables were used as ANN input variables: velocity, VSP, engine speed, engine torque, and engine coolant temperature.

Among the five input variables, the engine coolant temperature was the key parameter for estimating cold start emissions. Through trial and error, we found that ANN models using the engine coolant temperature as an input variable were able to predict the cold start effect on exhaust emissions. However, the prediction quality of emission models is affected not only by the engine coolant temperature, but also by other input variables, such as velocity, VSP, engine speed, and engine torque. Therefore, we developed four different ANN models to comprehensively analyze the performance of cold start emission models. The detailed descriptions of each ANN model are as follows:

- Vehicle model

velocity and VSP were used as inputs for the Vehicle model. Although this model cannot directly consider engine parameters, it was easy to use and practical because velocity and VSP are relatively easily available parameters. For example, EPA MOVES (USEPA, 2011), which is the vehicle emission inventory system of the U.S., uses velocity and VSP for emission estimation.

- Engine model
  Engine-related variables (engine speed and engine torque) were used as inputs for the Engine model. The engine speed and engine torque are used to represent the basic engine operating conditions. These two variables are widely used in vehicle-dynamics-based models for fuel and emission predictions (Rexeis, 2017; Ehsani et al., 2016; Srinivasan and Kothalikar, 2009). In contrast to the Vehicle model, the Engine model directly considers the engine operating conditions.
- Cold-vehicle model and Cold-engine model
  The 'Cold' models used the engine coolant temperature as an additional input variable, as compared to the Vehicle and Engine models. These models were designed to consider the cold start effect on exhaust emissions by considering temperature-related variables for emission prediction.

Except for the input layer, all ANN models had the same network structure. The hidden layer consists of three layers, and the first, second, and third layers contain 64, 128, and 128 neurons, respectively. Neurons in the hidden layers were fully connected, and a dropout layer was not used. The number of output variables for these ANN models was singular, and we trained separated ANN models to predict CO_2, NOx, CO, and THC emissions. Through the training, mean square propagation algorithm adjust the trainable parameters in all neurons. Although the number of trainable parameters is slightly depending on the number of ANN inputs, about 25,000 parameters were adjusted by the learning algorithms. For loss function, mean square error were used. In each hidden layer, the Relu function was used as an activation function.

2.2. ANN training data

RDE data of two diesel light-duty vehicles were used for ANN training. Table 1 shows the vehicle specifications of the two light-duty vehicles with 2000 cc diesel engine. The model year of Vehicle A is 2009, which is nine years older than Vehicle B. Since emission regulations have been updated over time, Vehicle B was subject to the Euro 6d-temp regulation, which is a more stringent emission regulation than the Euro 5 regulation of Vehicle A. Therefore, advanced emission reduction devices, such as a lean NOx trap (LNT) and selective catalytic reduction (SCR), were used in Vehicle B to meet the stricter emission standards. Although both vehicles have a similar engine size, Vehicle B was 170 kg heavier than Vehicle A due to the additional aftertreatment devices.

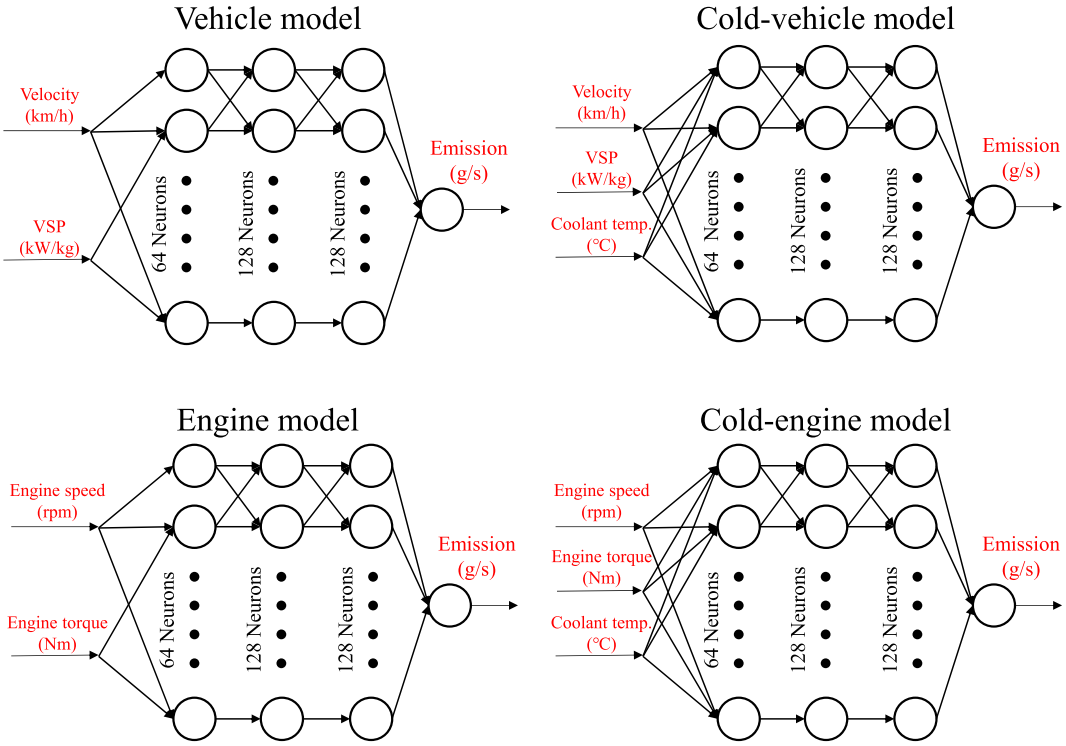

Fig. 1. Structures of artificial neural network models.

Table 1
Main characteristics of test vehicles.

	Emission regulation	Engine	Model year	Aftertreatment system	Curb weight	Amount of experimental data
Vehicle A	Euro 5	1955 cc diesel	2009	DOC, DPF	1875 kg	30,100 s (1 hot, 5 cold)
Vehicle B	Euro 6d-temp	2045 cc diesel	2018	LNT, DPF, SCR	2045 kg	30,411 s (2 hot, 3 cold)

In Korea, RDE testing is mandatory for diesel vehicles (Park et al., 2021), and the RDE data of this study were measured in compliance with the standard testing procedure. For Vehicles A and B, five and three cold start tests were conducted, respectively. In accordance with the RDE test standard, the velocity was controlled not to exceed 60 km/h during the first 5 min after starting. Therefore, high-velocity driving was rarely observed in the cold start phase.

The RDE data were divided into three parts for ANN training, validation, and performance testing. ANN models were trained using the training data set through machine learning. The validation dataset was used to inspect the occurrence of training errors, such as overfitting and divergence. Then, we validated the prediction accuracy of the trained ANN model based on the data set of performance testing. For performance testing, 1000 s of continuous data after the engine started were selected from the whole data set. Except for the performance testing data, remaining data were randomly divided into training and validation sets at an 8:2 ratio.

The ANN training data were measured from the vehicle tests. During the RDE test, vehicle operating variables (velocity, engine speed, engine torque, engine coolant temperature) were collected through the on-board diagnostics (OBD) system. Instantaneous CO_2, NOx, CO, and THC emissions were measured with a portable emission measurement system (PEMS). However, due to some experimental failure, CO emissions of Vehicle A and THC emissions of Vehicle B were not measured.

In addition, we calculated VSP based on the measured velocity and simple vehicle specifications. VSP represents the required specific power for a vehicle to operate under certain driving conditions, such as the velocity and road gradient. VSP was calculated as follows.

$$VSP = \frac{A \cdot v + B \cdot v^2 + C \cdot v^3 + m \cdot a \cdot v}{m} \quad (1)$$

Here, VSP is the vehicle specific power (W/kg); v is the vehicle velocity (m/s); A is the rolling resistance term (W/(m/s)); B is the friction term (W/(m/s)^2); C is the aerodynamic drag term (kW/(m/s)^3); m is the vehicle mass (kg); and a is the vehicle acceleration (m/s^2).

In order to increase the training efficiency, the ranges of the five ANN input variables (velocity, VSP, engine speed, engine torque, engine coolant temperature) were scaled by standardization, as follows.

$$x_{scaled} = \frac{x - x_{mean}}{x_{stdev}} \quad (2)$$

Here, x_{scaled} is the standardized value; x represents the ANN input variable (velocity, VSP, engine speed, engine torque, engine coolant temperature), x_{mean} is the mean of x; and x_{stdev} is the standard deviation of x.

2.3. Development of emission maps

Since the ANN model is a black box model, we cannot directly describe the trained emission characteristics in the ANN model. In this study, cold start emission characteristics were visually described in the form of emission maps. The emission map graphically showed the correlations between the operating variables and exhaust gas emissions. Depending on the number of input variables of the ANN models, emission maps were developed in a three-dimensional (two input variables, one output variable) or four-dimensional (three input variables, one output variable) data form. In order to investigate cold emission characteristics, emission maps according to engine coolant temperature were compared.

In addition to being used to visualize the emission characteristics, emission maps were used to predict exhaust emissions. The instantaneous mass flow rate of the exhaust emission was calculated using an interpolation function based on the emission map. By comparing experimental emissions and predicted emissions, we validated the emission map-based prediction accuracy.

2.4. Evaluating the effects of cold start conditions on exhaust emissions

Based on the developed emission map, we estimated vehicle emissions using the performance testing data, which was not used for ANN training. By comparing the predicted emissions and experimental emissions, the prediction accuracy was validated. We used the 'scatter interpolant' function of MATLAB, which performed interpolation based on Delaunay triangulation of the data points of the emission map (Amidror, 2002). In light of practicality and applicability, we use emission maps with interpolation functions for emission prediction rather than directly running the trained ANN model for emission predictions. Since an emission map is composed of a data table, it can be easily used and incorporated with other tools without needing to use the trained ANN model.

In addition to the validation analysis, cold start emissions were estimated under three temperature scenarios to quantitatively analyze the cold start effect on exhaust emissions. Fig. 2(a) shows the engine coolant temperature rise of Vehicles A and B in cold start conditions with an ambient temperature of 15 to 25 °C. After the engine start, the engine coolant temperature begins to rise at a temperature similar to the ambient conditions and stabilized around 90 °C. The engine coolant temperatures of Vehicle A and B started from 30 °C and 60 °C, respectively. Due to some experimental issues, the engine coolant temperature of Vehicle A was measured from 60 °C.

However, under various ambient temperature conditions, the engine coolant temperature rises more quickly or slowly than what is shown in Fig. 2(a). In order to consider the effects of various cold start conditions on exhaust emissions, we evaluated vehicle emissions under three engine coolant temperature scenarios. The temperature rise rate was set differently for the three cold start conditions, as shown in Fig. 2(b). The engine coolant temperature of the normal scenario was similar to the experimental data in Fig. 2(a). The gradients of the engine coolant temperature lines of the fast rise, normal, and slow rise conditions were set to 0.75, 1, and 1.5 °C/s, respectively. The engine coolant temperature rises to 85 °C and then stabilized in this temperature without fluctuation.

3. Results

3.1. Emission maps

In order to visualize the emission characteristics of the ANN models, we developed emission maps, which represent exhaust emissions as a function of the operating variables, such as the velocity, VSP, engine speed, engine torque, and engine coolant temperature. According to

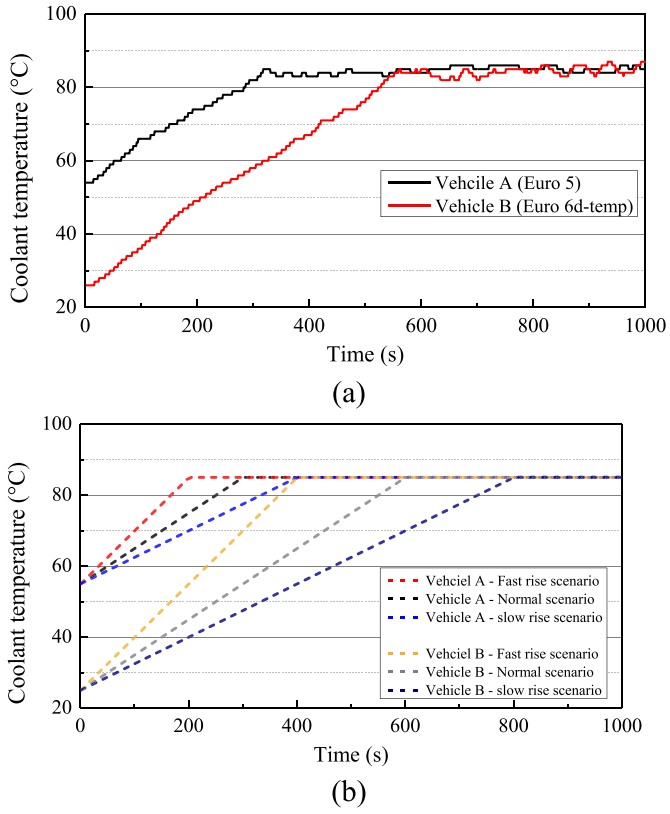

Fig. 2. Engine coolant temperature: (a) experimental data and (b) three temperature rise scenarios.

the input variables of each ANN model, we developed CO_2, NOx, THC, and CO emission maps for Vehicles A and B.

For two-variable input models, such as the Vehicle model and Engine model, we visualized the emission characteristics in a single contour graph (x-axis: first operating variables, y-axis: second operating variables, z-axis: mass flow rate of exhaust gas). On the contrary, in the case of the Cold-vehicle model and Cold-engine model, which use three variables as model inputs, multiple emission maps were developed according to the engine coolant temperature. For Vehicles A and B, emission maps were analyzed for engine coolant temperatures ranging from 60 to 90 °C and 30 to 90 °C, respectively. Due to experimental issues, emission data in the lower temperature range (30 to 60 °C) of Vehicle A were not measured.

Fig. 3 shows the CO_2 emission map of Vehicle A. In the Vehicle model map, dynamic emission characteristics as a function of the vehicle operating conditions were observed. In the positive VSP region (acceleration or cruising), CO_2 emissions increased as velocity and VSP increased. On the contrary, in the negative VSP region (deceleration), velocity and CO_2 emissions were not proportional. In the Cold-vehicle model maps at engine coolant temperatures of 60 °C and 75 °C, CO_2 emissions in the high-velocity region were quite low. This result was due to the absence of training data at the high-velocity and low-engine coolant temperature condition. Although ANN model can predict emissions in all range of operating area, the prediction accuracy for the outside of the training data is not reliable. In the RDE test, the velocity was controlled to avoid exceeding 60 km/h for 5 min after cold start, so the experimental data of the high-velocity and low-engine coolant temperature region were not acquired. Therefore, ANN training in this region was not properly conducted, resulting in an abnormal CO_2 mass flow rate in the emission map, and predicting emissions outside the training data should be avoided.

On the contrary, abnormal CO_2 emissions were not observed in the Cold-engine model map in the low-temperature condition. Although the vehicle velocity was controlled below 60 km/h in the experiment, the engine speed and engine torque were not restricted to a narrow range because of the influence of gear shifting at the transmission. Therefore, ANN training was properly conducted for the overall engine operating range. In the Cold-engine model map, noticeable differences in CO_2 emissions at different engine coolant temperature conditions were not shown, and CO_2 emissions were not significantly affected by the engine coolant temperature.

As shown in Fig. 4, the overall shape of the CO_2 emission map of Vehicle B was relatively twisted compared to that of Vehicle A. Since Vehicle B uses advanced emission reduction technologies, such as LNT and SCR, the emission characteristics of Vehicle B were more complicated than those of Vehicle A, resulting in a relatively curved contour line in the emission map. For the Cold-vehicle model map and Cold-engine model map, significant differences in the CO_2 emissions were not observed for different engine coolant temperature conditions.

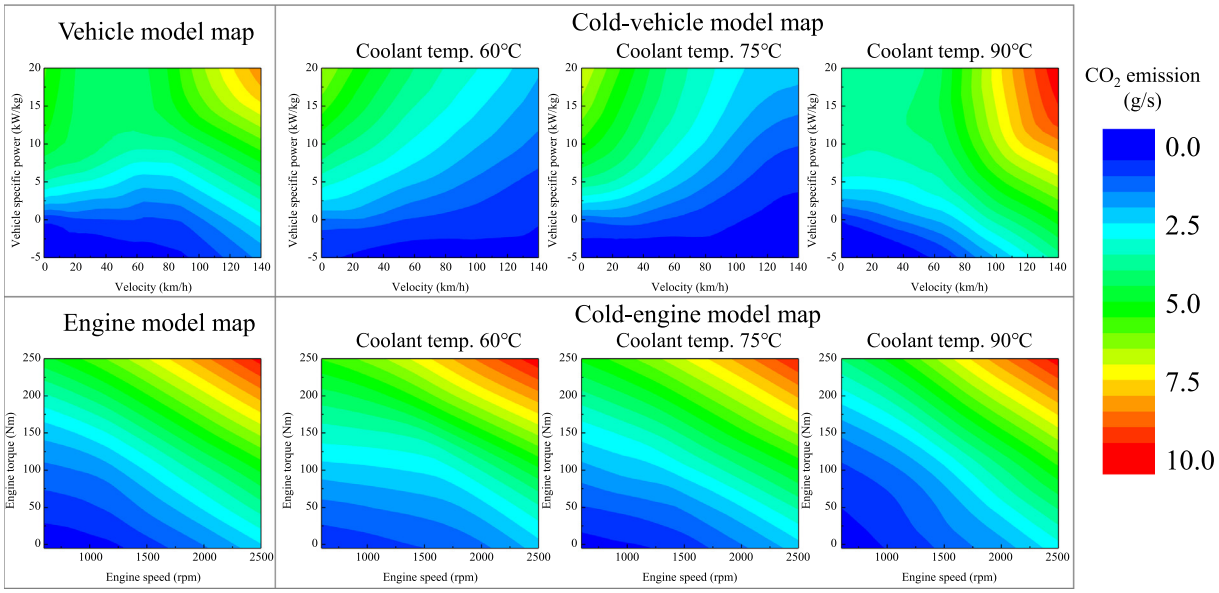

Fig. 3. CO_2 emission maps of Vehicle A.

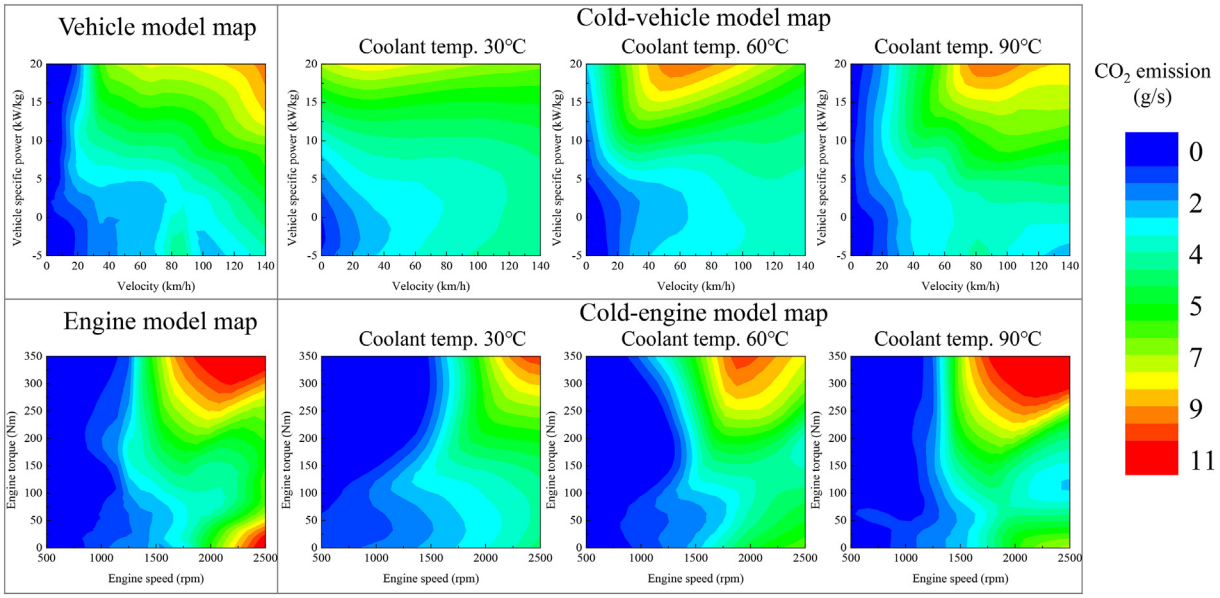

Fig. 4. CO_2 emission maps of Vehicle B.

Fig. 5 illustrates the NOx emission map of Vehicle A. The overall shape of the NOx emission map was similar to the CO_2 emission map of Vehicle A. In both the Cold-vehicle map and Cold-engine map, NOx emissions in the cold start condition (engine coolant temperatures of 60 °C and 75 °C) were not high compared to the warmed-up condition (engine coolant temperature of 90 °C). In the case of the Cold-engine model map, NOx emissions did not vary significantly with different engine coolant temperatures, and NOx emissions increased as the engine speed and engine torque increased.

In contrast to Vehicle A, NOx emissions of Vehicle B increase as the engine coolant temperature decreases, as shown in Fig. 6. For both the Cold-vehicle model map and Cold-engine model map, NOx emissions at low-temperature conditions (emission map with coolant temperatures of 30 °C and 60 °C) were higher than at the warmed-up driving condition (emission map with a coolant temperature of 90 °C). Since Vehicle B was equipped with LNT and SCR, a minimum temperature was required for aftertreatment devices to initiate the catalytic reaction properly. However, right after the cold start, the NOx reduction efficiency is low due to the low temperature of the aftertreatment device, resulting in the high NOx emission rate in the emission map. On the contrary, the Vehicle model and Engine model could not consider the cold start effect on NOx emissions, because the engine coolant temperature dose was not taken into account in these emission maps.

The cold start effect on the THC emissions of Vehicle A is shown in Fig. 7. The THC emissions and engine coolant temperature were inversely proportional. In the cold start phase, hydrocarbons contained in the fuel could not be sufficiently oxidized due to the deteriorated fuel atomization, resulting in increased THC emissions (Bielaczyc and Merkisz, 1997). In addition, the performance of the aftertreatment devices for THC reduction was not effective at low temperatures. These emission characteristics are clearly observed in the emission maps of the Cold-vehicle model and Cold-engine model.

Fig. 8 shows the CO emission maps of Vehicle B. The emission characteristics of CO were similar to the THC emissions in that the emissions were high at low engine coolant temperatures. High CO emissions were observed in the Cold-vehicle model map and Cold-engine model map at

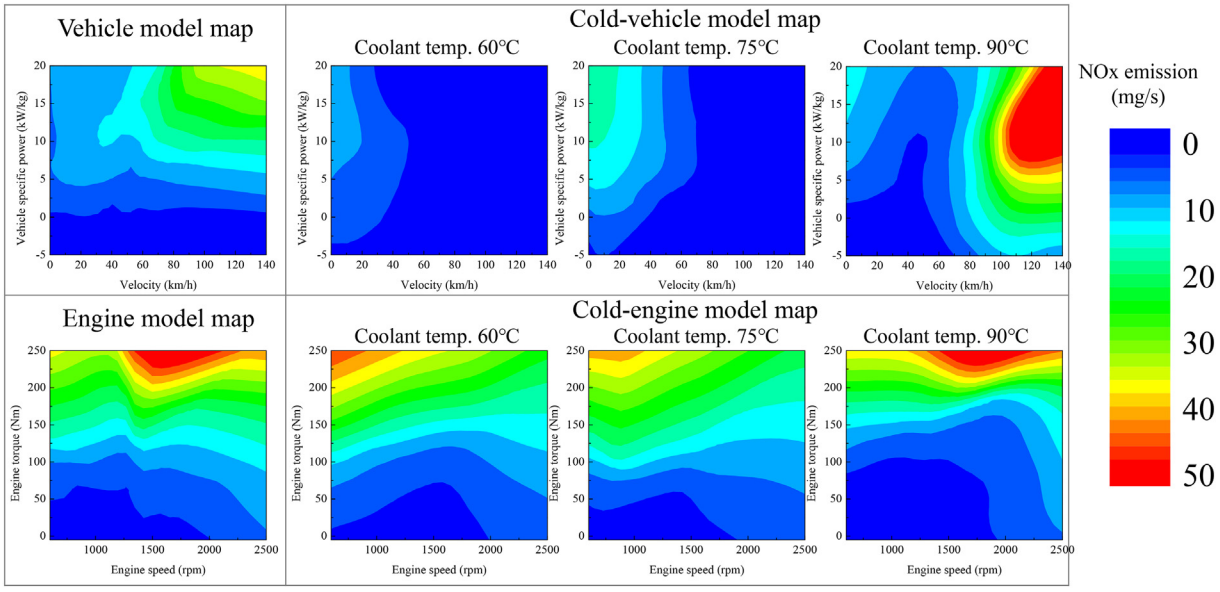

Fig. 5. NOx emission maps of Vehicle A.

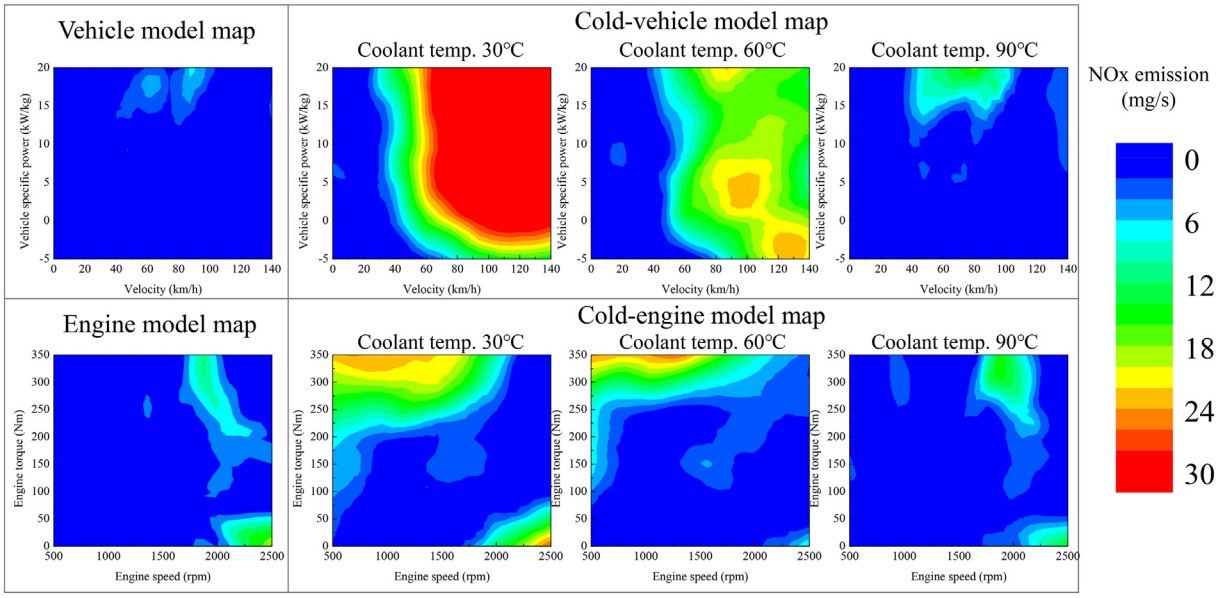

Fig. 6. NOx emission maps of Vehicle B.

low engine coolant temperatures. However, the Vehicle model and Engine model, which did not use the engine coolant temperature as a map variable, could not take into account the cold start characteristics. These models could not distinguish the cold start phase. Emission maps of these two models only represent the warmed-up emission characteristics, rather than represent the cold start emissions. Since the cold start phase is a small part (less than 10%) of the total vehicle test data, cold emission characteristics were suppressed during the training of the Vehicle model and Engine model.

3.2. Cold start emission predictions based on emission maps

We predicted vehicle emissions during the 1000 s after the cold start using the emission maps. The performance dataset, which was not used for ANN training, was used to predict emissions. By comparing the predicted results with experimental data, the prediction accuracy of proposed method was validated.

The comparison of the experimental emissions and predicted emissions is shown in Fig. 9. Noticeable cold start effects were not observed in the CO_2 emissions of Vehicles A and B and the NOx emissions of Vehicle A. For the CO_2 emissions shown in Fig. 9 (a) and (b), four types of emission maps of Vehicles A and B well predicted the experimental values. Since the cold start effect on CO_2 emissions was not significant, the CO_2 prediction results of Cold-vehicle model and Cold-engine model were similar to that of the Vehicle model and Engine model.

Similarly, significant cold start effects on the NOx emissions of Vehicle A were not observed in Fig. 9(c). On the contrary, for Vehicle B, a sharp increase in NOx emissions during the cold start phase occurred after 400 s, as shown in Fig. 9(d). Since the NOx conversion efficiencies of SCR and LNT (mounted on Vehicle B) were deteriorated at low temperatures, NOx reduction was not sufficiently performed in the cold start phase, resulting in a sharp increase of NOx emissions. Although the conversion efficiency of the NOx reduction device was low in the whole period of cold start condition, the amount of NOx emission before 400 s was not

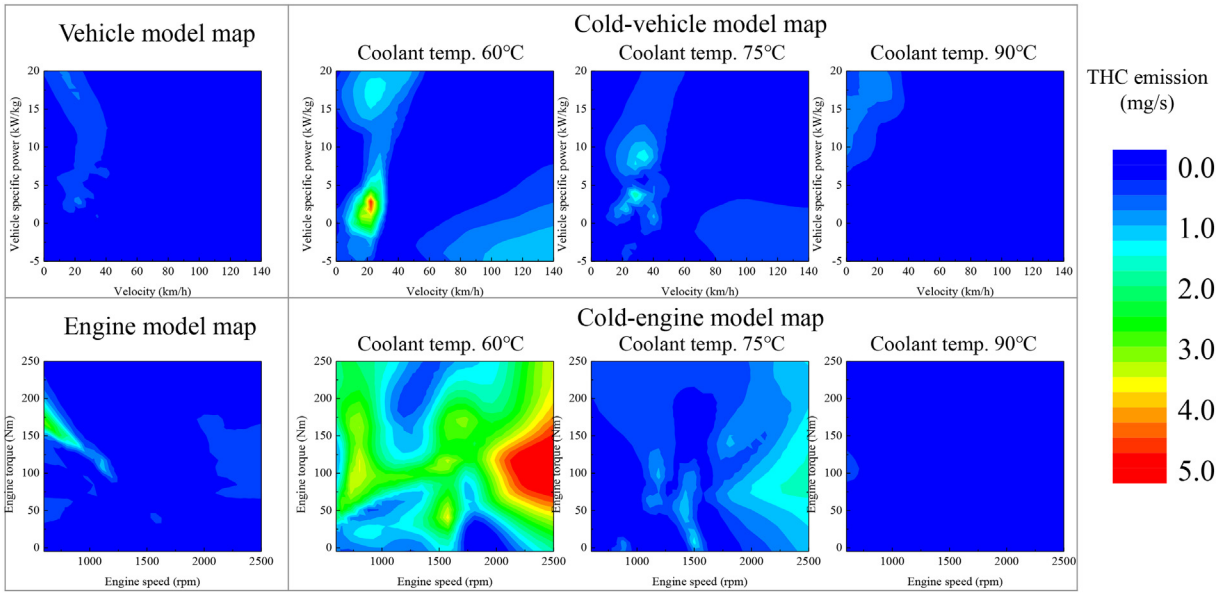

Fig. 7. THC emission maps of Vehicle A.

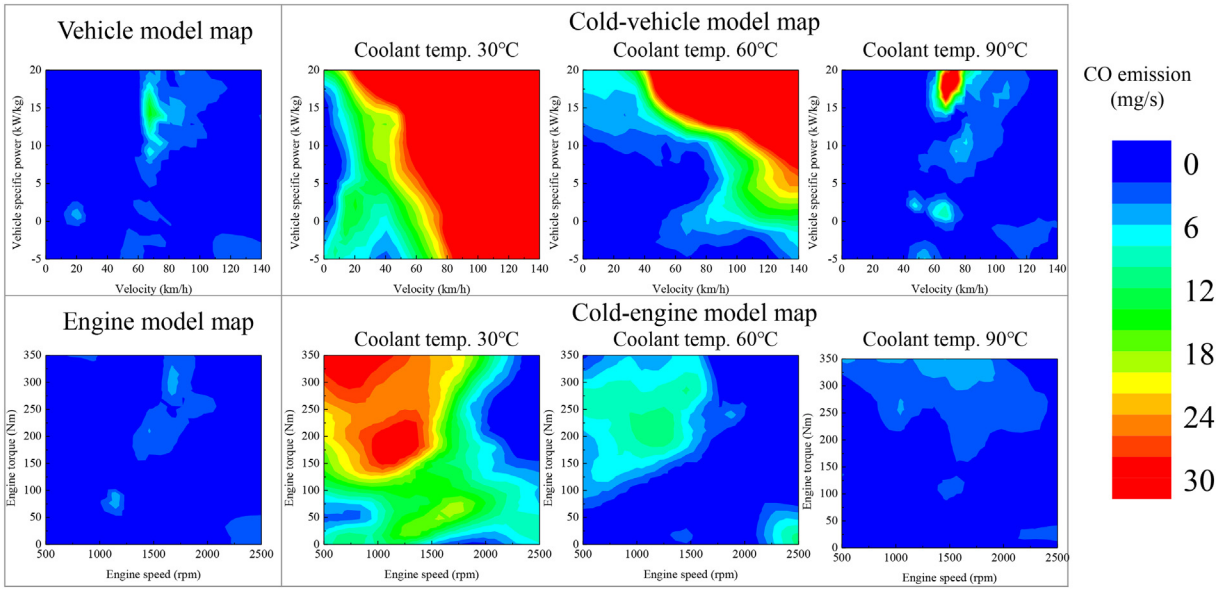

Fig. 8. CO emission maps of Vehicle B.

significant because vehicle and engine were operated at low speed and low load conditions. As shown in Cold-vehicle model and Cold-engine model map in Fig. 6, the NOx emissions in low speed and low load area are small. After 400 s, engine and vehicle operated at higher speed and higher load condition than before, but the aftertreatment devices was not fully heated due to cold start, resulting in sharp increase in NOx emission. Since Vehicle and Engine models used temperature-independent variables as model input, cold start emission characteristics were unpredictable and only consider emissions in warmed-up conditions, as previously shown in the emission maps in Fig. 6. On the other hand, the Cold-

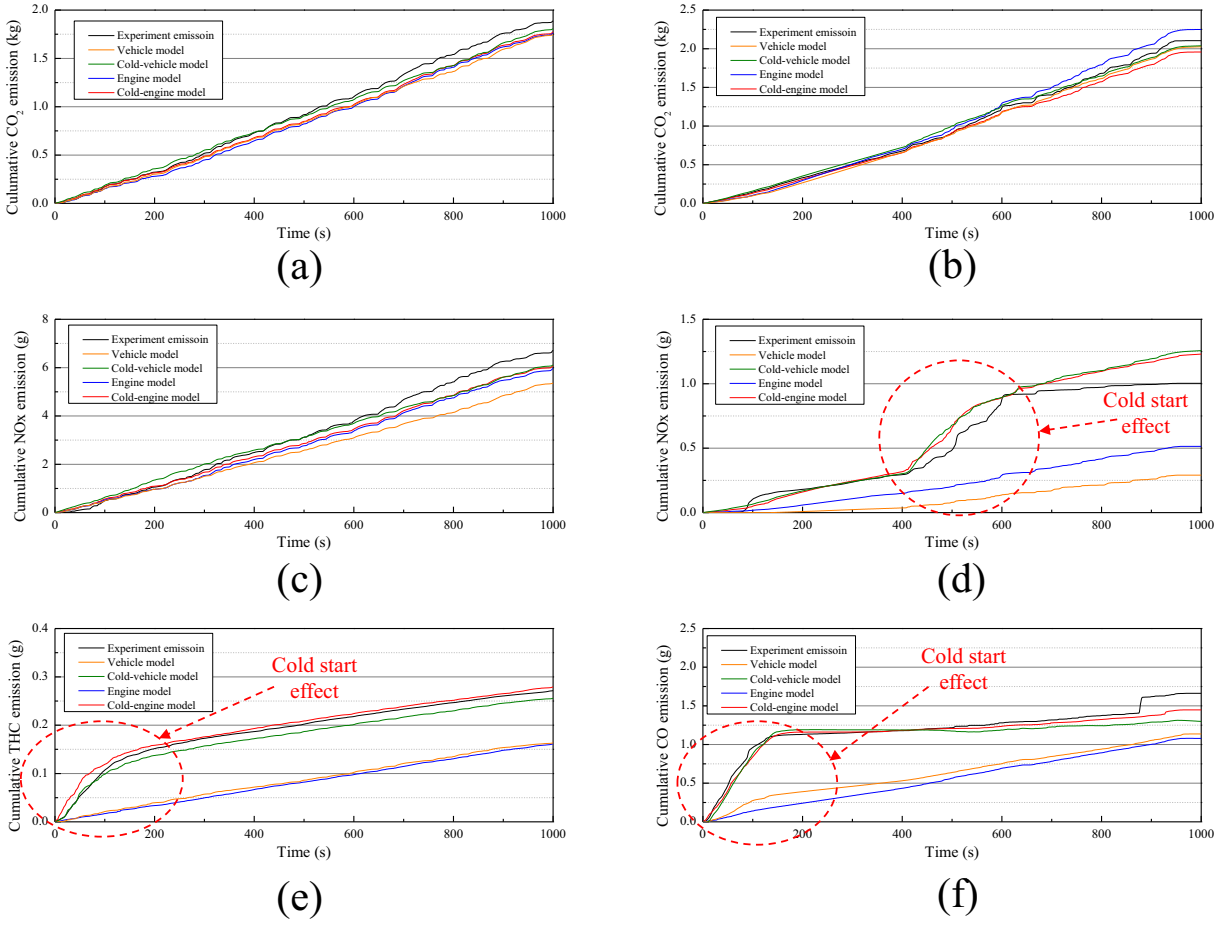

Fig. 9. Comparison of experimental emissions and ANN-predicted emissions: (a) CO_2 emissions of Vehicle A, (b) CO_2 emissions of Vehicle B, (c) NOx emissions of Vehicle A, (d) NOx emissions of Vehicle B, (e) THC emissions of Vehicle A, and (f) CO emissions of Vehicle B.

vehicle model and Cold-engine model are able to accurately predict NOx emissions, including the sharp increase. Similar tendencies were observed in the THC and CO prediction results in Fig. 9 (e) and (f).

Similar to the Vehicle and Engine models of this study, there have been attempts to predict vehicle emissions by using temperature-independent variables as model input such as speed, VSP, engine speed, and engine torque (Le Cornec et al., 2020, Wang et al., 2018, Hashemi and Clark, 2007, Jaikumar et al., 2017). However, these models were unable to predict cold start emissions due to the absence of consideration of temperature-related variables for emission estimation. On the contrary, Cold-vehicle model and Cold-engine model well predicted cold start emission by considering engine coolant temperature as model input.

3.3. Cold start emissions under different temperature rise scenarios

In order to quantitatively analyze the cold start effect on exhaust emissions, we predict emissions using the Cold-engine model in three engine coolant temperature scenarios, as shown in Fig. 2(b). The predicted results are illustrated in Fig. 10. For CO_2 emission of Vehicles A and B, as well as NOx emissions of Vehicle A, the cold start emissions were not significantly affected by the temperature condition. However, other emissions (NOx emissions of Vehicle B, THC emissions of Vehicle A, and CO emissions of Vehicle B) were sensitive to the temperature conditions. The exhaust emissions increased under the slow temperature rise scenario, while emissions decreased under higher engine coolant temperature conditions. Fig. 11 summarizes the predicted results for the three engine coolant temperature scenarios. These results shows that the proposed methodology comprehensively considered the effect of the vehicle characteristics, emission types, and temperature conditions on cold start emissions.

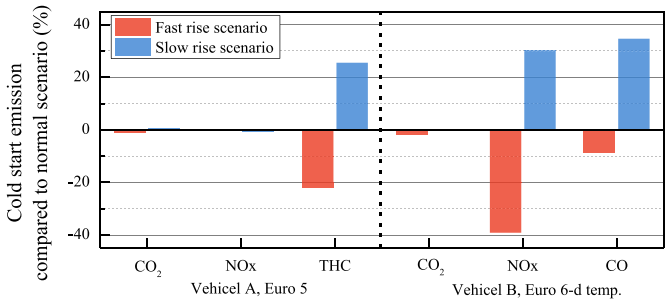

Fig. 11. Summary of the cold start effect at different temeprature conditions.

4. Discussion and conclusion

In this study, we estimated cold start emissions based on emission maps and an artificial neural network model. Through machine learning, the emission characteristics presented in real-world driving data were trained at artificial neural network models. As input variables for the models, the velocity, vehicle specific power, engine speed, engine torque, and engine coolant temperature were used to estimate the carbon dioxide, nitrogen oxides, total hydrocarbon, and carbon monoxide emissions of diesel passenger vehicles. Four types of artificial neural network models were developed according to the combination of input variables, and the prediction accuracy of cold start emissions was significantly improved when the engine coolant temperature was used as a model input. By considering the engine coolant temperature as a key variable, we visualized emission characteristics for different

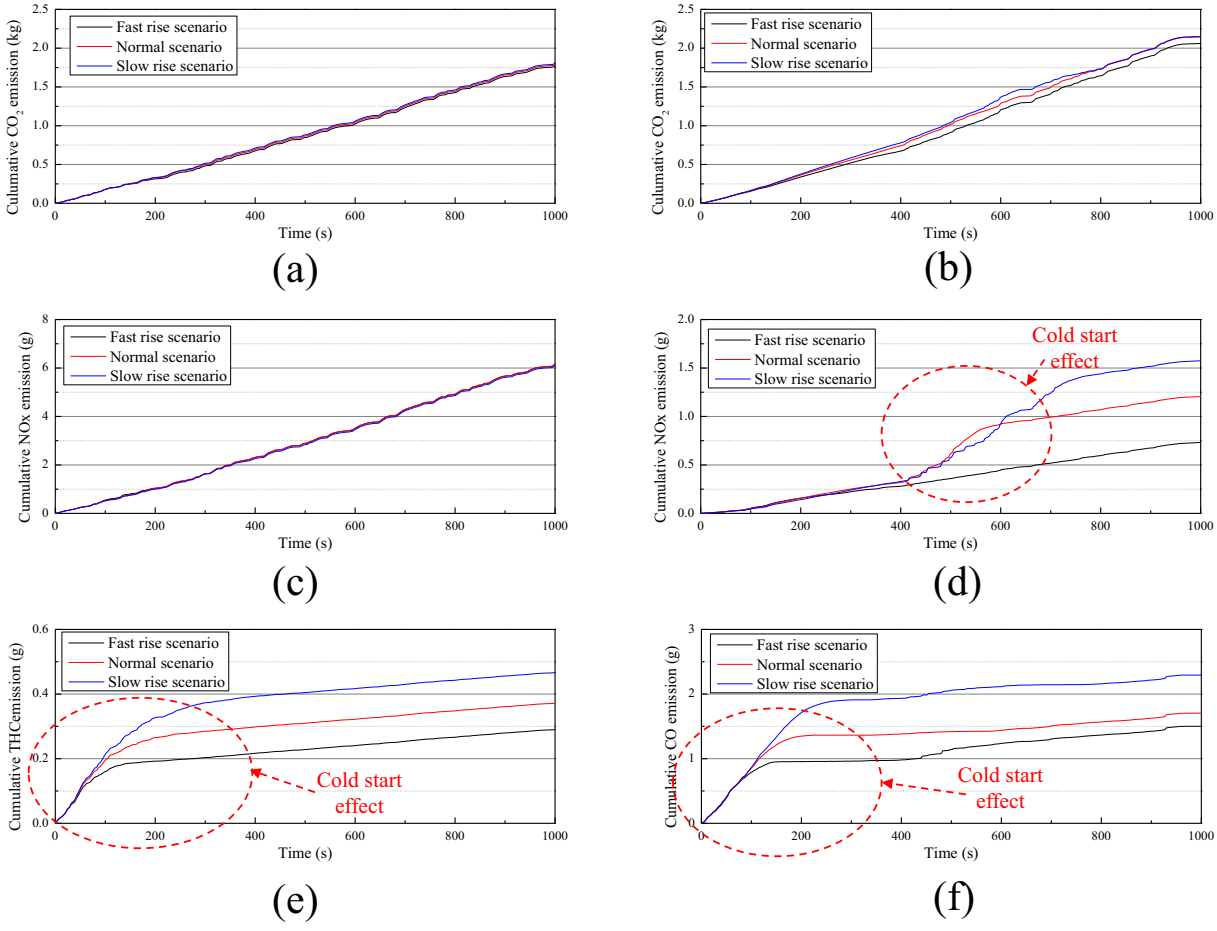

Fig. 10. Cold start emissions under three temperature rise scenarios: (a) CO_2 emissions of Vehicle A, (b) CO_2 emissions of Vehicle B, (c) NOx emissions of Vehicle A, (d) NOx emissions of Vehicle B, (e) THC emissions of Vehicle A, and (f) CO emissions of Vehicle B.

engine coolant temperatures in the form of emission maps. The proposed models (Cold-vehicle model and Cold-engine model) predicted cold start emissions with high accuracy.

Since the cold start effect on carbon dioxide emissions was insignificant, a relatively simple model that did not consider cold emission characteristics is sufficient to accurately predict the carbon dioxide emissions. However, nitrogen oxides emission sensitivity to cold start operation was quite different depending on the vehicle type. In the case of Vehicle A, nitrogen oxides emissions did not change significantly, regardless of the engine coolant temperature condition; this was similar to the carbon dioxide emission characteristics. However, nitrogen oxides emissions of Vehicle B increased under cold temperature conditions due to the low nitrogen oxides conversion efficiency of SCR and LNT. The Cold-vehicle model and Cold-engine model accurately predicted the sharp increase in Nitrogen oxides emissions during the cold start phase of Vehicle B. In the case of carbon monoxide and total hydrocarbon emissions, rapid increases in emissions were observed during the cold start phase. These emission characteristics were well predicted in the Cold-vehicle model and Cold-engine model, while the Vehicle model and Engine model were unable to predict the cold start carbon monoxide and total hydrocarbon emissions.

In addition to the emission predictions, we quantitatively analyzed the cold start effect on exhaust emissions according to three engine coolant temperature scenarios. As expected, Nitrogen oxides emissions of Vehicle A and carbon dioxide emissions were only slightly affected by the temperature conditions. In the case of temperature-sensitive exhaust gases, such as Nitrogen oxides emissions of Vehicle B and carbon monoxide and total hydrocarbon emissions, the amount of emissions was inversely proportional to temperature. Although, the results for different temperature assumptions were not validated using experimental data, the proposed models show the potential to consider cold start emissions in various temperature conditions.

As vehicle regulations have been strengthened over time, various technologies have been applied to vehicles for emission reduction, resulting in diversified emission characteristics depending on the vehicle and emission types. Most prior works have predicted vehicle emissions mainly in the warmed-up condition or predicted cold start emissions using complicated modeling approaches, which were inadequate and could not be applied to various types of vehicles. However, the proposed methodology of this study is a relatively simple methodology based on the artificial neural network model, and the prediction accuracy was satisfactory. The notable advantage of this approach is that it predicts the cold start emissions with high accuracy, regardless of the vehicle and emission types. We believe that the proposed model can overcome the shortcomings of conventional emission models.

This methodology is useful for assessing transportation emissions in urban areas where cold start emissions account for a significant percentage of pollutant emissions due to the high frequency of cold starts in these areas. Since we predicted carbon dioxides, nitrogen oxides, carbon monoxide, and total hydrocarbon emissions of diesel vehicles in this study, future work should also investigate the emission prediction of other powertrains, such as SI engines and hybrid vehicles, as well as other types of emissions, such as particulates.

CRediT authorship contribution statement

Jigu Seo: Writing- Original draft preparation, Conceptualization, Methodology, Investigation, Experiments. **Sungwook Park:** Writing-Reviewing and Editing, Supervision.

Declaration of competing interest

The authors declare that they have no known competing financial interests or personal relationships that could have appeared to influence the work reported in this paper.

Acknowledgement

This work was supported by National Institute of Environmental Research (NIER) of the Republic of Korea (grant number: NIER-RP2020-131) and BK21 FOUR Program.

References

Amidror, Isaac, 2002. Scattered data interpolation methods for electronic imaging systems: a survey. J. Electron. Imaging 11 (2), 157–176. https://doi.org/10.1117/1.1455013.

Bielaczyc, Piotr, Merkisz, Jerzy, 1997. Exhaust emission from passenger cars during engine cold start and warm-up. SAE Technical Paper.

Bielaczyc, P., Szczotka, A., Woodburn, J., 2011. The effect of a low ambient temperature on the cold-start emissions and fuel consumption of passenger cars. Proc. Inst. Mech. Eng. Part D-J. Automob. Eng. 225 (9), 1253–1264. https://doi.org/10.1177/0954407011406613.

Cornec, Le, Clémence, M.A., Molden, Nick, van Reeuwijk, Maarten, Stettler, Marc E.J., 2020. Modelling of instantaneous emissions from diesel vehicles with a special focus on NOx: insights from machine learning techniques. Sci. Total Environ. 737, 139625. https://doi.org/10.1016/j.scitotenv.2020.139625.

Dardiotis, Christos, Martini, Giorgio, Marotta, Alessandro, Manfredi, Urbano, 2013. Low-temperature cold-start gaseous emissions of late technology passenger cars. Appl. Energy 111, 468–478. https://doi.org/10.1016/j.apenergy.2013.04.093.

Du, Baocheng, Zhang, Li, Geng, Yangtao, Zhang, Yun, Hualong, Xu., Xiang, Gan, 2020. Testing and evaluation of cold-start emissions in a real driving emissions test. Transport. Res. DTransport. Environ. 86, 102447. https://doi.org/10.1016/j.trd.2020.102447.

Ehsani, Mehrsa, Ahmadi, Abbas, Fadai, Dawud, 2016. Modeling of vehicle fuel consumption and carbon dioxide emission in road transport. Renew. Sust. Energ. Rev. 53, 1638–1648. https://doi.org/10.1016/j.rser.2015.08.062.

Favez, Jean-Yves, Weilenmann, Martin, Stilli, Jan, 2009. Cold start extra emissions as a function of engine stop time: evolution over the last 10 years. Atmos. Environ. 43 (5), 996–1007. https://doi.org/10.1016/j.atmosenv.2008.03.037.

Franco, Vicente, Kousoulidou, Marina, Muntean, Marilena, Ntziachristos, Leonidas, Hausberger, Stefan, Dilara, Panagiota, 2013. Road vehicle emission factors development: a review. Atmos. Environ. 70, 84–97. https://doi.org/10.1016/j.atmosenv.2013.01.006.

Gao, Jianbing, Tian, Guohong, Sorniotti, Aldo, Karci, Ahu Ece, Di Palo, Raffaele, 2019. Review of thermal management of catalytic converters to decrease engine emissions during cold start and warm up. Appl. Therm. Eng. 147, 177–187. https://doi.org/10.1016/j.applthermaleng.2018.10.037.

Gao, Jianbing, Chen, Haibo, Liu, Ye, Laurikko, Juhani, Li, Ying, Li, Tiezhu, Ran, Tu., 2021. Comparison of NOx and PN emissions between euro 6 petrol and diesel passenger cars under real-world driving conditions. Sci. Total Environ. 801, 149789. https://doi.org/10.1016/j.scitotenv.2021.149789.

Giannelli, Robert Anthony, Stubleski, Ryan, Saunders, Anthony, 2014. Semi-empirical analysis of cold start emissions. SAE Int. J. Fuels Lubr. 7 (2), 591–599. https://doi.org/10.4271/2014-01-1619.

Gkatzoflias, Dimitrios, Kouridis, Chariton, Ntziachristos, Leonidas, Samaras, Zissis, 2007. COPERT 4. Computer Programme to Calculate Emissions From Road Transport-Users Manua. European Environment Agency, European Topic Centre on Air Air and Climate Change (ETC-ACC), Copenhagen.

Hashemi, Nastaran, Clark, N.N., 2007. Artificial neural network as a predictive tool for emissions from heavy-duty diesel vehicles in Southern California. Int. J. Engine R 8 (4), 321–336. https://doi.org/10.1243/14680874JER00807.

Jaikumar, Rohit, Shiva Nagendra, S.M., Sivanandan, R., 2017. Modeling of real time exhaust emissions of passenger cars under heterogeneous traffic conditions. Atmos. Pollut. Res. 8 (1), 80–88. https://doi.org/10.1016/j.apr.2016.07.011.

Joumard, Robert, André, Jean-Marc, Rapone, Mario, Zallinger, Michael, Kljun, Natascha, André, Michel, Samaras, Zissis, Roujol, Stéphane, Laurikko, Juhani, Weilenmann, Martin, 2007. Emission factor modelling and database for light vehicles. Available atArtemis Deliverable, p. 3. https://hal.archives-ouvertes.fr/hal-00916945/document.

Neely, Gary D., Sarlashkar, Jayant V., Mehta, Darius, 2013. Diesel cold-start emission control research for 2015–2025 LEV III emissions. SAE Int. J. Engines 6 (2), 1009–1020. https://doi.org/10.4271/2013-01-1301.

Neely, Gary D., Mehta, Darius, Sarlashkar, Jayant, 2014. Diesel cold-start emission control research for 2015–2025 LEV III emissions-part 2. SAE Int. J. Engines 7 (3), 1302–1310. https://doi.org/10.4271/2014-01-1552.

Park, Junhong, Shin, Myunghwan, Lee, Jongchul, Lee, Jongtae, 2021. Estimating the effectiveness of vehicle emission regulations for reducing NOx from light-duty vehicles in Korea using on-road measurements. Sci. Total Environ. 767, 144250. https://doi.org/10.1016/j.scitotenv.2020.144250.

Rexeis, Martin, 2017. VECTO tool development: Completion of methodology to simulate Heavy Duty vehicles' fuel consumption and CO2 emissions Upgrades to the existing version of VECTO and completion of certification methodology to be incorporated into a Commission legislative proposal. https://ec.europa.eu/clima/sites/clima/files/transport/vehicles/docs/sr7_lot4_final_report_en.pdf.

Roberts, Andrew, Brooks, Richard, Shipway, Philip, 2014. Internal combustion engine cold-start efficiency: a review of the problem, causes and potential solutions. Energy Conv. Manag. 82, 327–350. https://doi.org/10.1016/j.enconman.2014.03.002.

Robinson, Kevin, Ye, Shifei, Yap, Yeow, Kolaczkowski, Stan T., 2013. Application of a methodology to assess the performance of a full-scale diesel oxidation catalyst during cold and hot start NEDC drive cycles. Chem. Eng. Res. Des. 91 (7), 1292–1306. https://doi.org/10.1016/j.cherd.2013.02.022.

Sabatini, Stefano, Kil, Irfan, Dekar, Joseph, Hamilton, Travis, Wuttke, Jeff, Smith, Michael A., Hoffman, Mark A., Onori, Simona, 2015. A new semi-empirical temperature model for the three way catalytic converter. IFAC-PapersOnLine 48 (15), 434–440. https://doi.org/10.1016/j.ifacol.2015.10.062.

Sharma, N., Chaudhry, K.K., Rao, C.V., 2005. Vehicular pollution modeling using artificial neural network technique: a review. Available at:J. Sci. Ind. Res. 64, 637–647. http://nopr.niscair.res.in/bitstream/123456789/5155/1/JSIR%2064%289%29%20637-647.pdf.

Srinivasan, P., Kothalikar, U.M., 2009. Performance fuel economy and CO 2 prediction of a vehicle using AVL Cruise simulation techniques. SAE Tech. Pap No. 2009-01-1862 https://doi.org/10.4271/2009-01-1862.

USEPA, 2011. Development of Emission Rates for Light-duty Vehicles in the Motor Vehicles Emissions Simulator (moves2010) Tech Rep EPA-420-R-11- 011. Available at Environmental Protection Agency, Washington DC. http://www3.epa.gov/otaq/models/moves/documents/420r11011.pdf.

Wang, Chao, Ye, Zhirui, Yongbo, Yu., Gong, Wei, 2018. Estimation of bus emission models for different fuel types of buses under real conditions. Sci. Total Environ. 640–641, 965–972. https://doi.org/10.1016/j.scitotenv.2018.05.289.

Weilenmann, Martin, Favez, Jean-Yves, Alvarez, Robert, 2009. Cold-start emissions of modern passenger cars at different low ambient temperatures and their evolution over vehicle legislation categories. Atmos. Environ. 43 (15), 2419–2429. https://doi.org/10.1016/j.atmosenv.2009.02.005.

Weilenmann, Martin F., Soltic, Patrik, Hausberger, Stefan, 2013. The cold start emissions of light-duty-vehicle fleets: a simplified physics-based model for the estimation of CO2 and pollutants. Sci. Total Environ. 444, 161–176. https://doi.org/10.1016/j.scitotenv.2012.11.024.